Iraqi J. Laser, Part A, Vol. 13, pp. 19-28 (2014)

IRAQI
JOURNAL
OF
LASER

Laser Induced Fluorescence Spectroscopy of Decamethylrhenocene $(\eta^5 - C_5 Me_5)_2$ Re in Supersonic Jet

Harith J. Saleh

Institute of Laser for Postgraduate Studies, University of Baghdad, Baghdad, Iraq

(Received 3 December 2013; accepted 16 October 2014)

Abstract: In this paper we report the use of supersonic jet laser induced fluorescence (LIF) spectroscopy to facilitate the study of the spectra of some organometallic sandwich compounds particularly the metallocenes. The charge-transfer processes within these compounds, especially ligand to metal charge transfer within decamethylrhenocene $(\eta^5 - C_5 Me_5)_2$ Re were of particular interest. The spectrum shows a high degree of structures, indicating that there are several levels populated and these molecules are able to undergo many possible transitions.

Introduction

The progress of high resolution spectroscopic studies of large molecules had been hindered by spectral complexity. Some of these complexities came from the fact that a large polyatomic molecule has a large number of vibrational degrees of freedom [4,5]. Another complication was due to the thermal distribution of molecules over many ground-state vibrational levels, which causes many hot bands to generate in the spectrum. Also the collisions between molecules in gas and condensed phases would play major roles in broadening of spectral bands. All these complicating factors become increasingly significant as a molecule is getting bigger. Eventually, the spectrum becomes a continuous feature, even in the gas phase.

The development of the supersonic jet technique has successfully solved the above problem. Supersonic expansion of sample molecules, seeded in high pressure rare gas, into a vacuum through a small nozzle orifice produces a supersonic jet in which the molecule is cooled by the collision-induced transfer of the thermal energy of molecule into the translational energy of the rare gas atoms [6,8]. The molecules in the supersonic jet are in a non-equilibrium state, and the temperature of the molecules is generally different for the translational, rotational, and vibrational degrees of freedom. In general, large polyatomic molecules having many low frequency vibrational modes are efficiently cooled and the vibrational temperature becomes very low. Therefore, the molecules are nearly all in the zero-point level of the ground state, and they are also in a collision-free condition. As a result, the two factors leading to the spectral congestion of large molecules- the appearance of hot bands and the collisional broadening - are almost completely removed, and sharp spectral features show up even for large molecules that ordinarily gives a continuous spectrum[9].

So far, for spectral measurements, there are two methods that are widely used;

1- Fluorescence excitation spectroscopy in which the electronic transition of a jet- cooled molecule is probed by the fluorescence emitted from the excited state reached by the transition.

2- Multi photon ionisation (MPI) spectroscopy, in which the transition is probed by the ions generated by resonance - enhanced multi-photon ionisation of a molecule.

In this work we are concerned with the use of fluorescence excitation spectroscopy to facilitate the study of the spectra of some organometallic compounds particularly the metallocenes. The charge-transfer processes within these compounds, especially ligand to metal charge transfer within decamethylrhenocene (η^5-$C_5Me_5)_2$ Re were of particular interest.

The electronic properties of this compound have been studied by different methods [1] for example visible absorption and laser- induced fluorescence in Ar and N_2 matrices, magnetic circular dichroism, electron spin resonance and gas phase photoelectron spectroscopy. No studies have been published on this compound.

The Electronic and Molecular Structure of Cp*Re

Cp^*_2Re is a stable molecule prepared by UV photolysis of the hydride Cp^*_2ReH. Cp^*_2 ReH is obtainable by condensation of rhenium vapour with C_5Me_5H. Briefly the synthesis of Cp^*_2Re is as follow:

Rhenium vapor (ca. 1.0 g) from a positive hearth electron beam furnace operating at 3200 °C was co-condensed with an excess of 1, 2, 3, 4, 5 – pentamethylcyclopentadiene in liquid nitrogen (T 77K). Work up of the reaction mixture and finally purification by sublimation afforded air-sensitive pale yellow crystals of bis (η–pentamethylcyclopentadienyl) rhenium hydride, (η-$C_5Me_5)_2$ Re H, in 15% yield (based on rhenium). Cp^*_2 Re H is a volatile air - sensitive crystalline solid, extremely soluble in hydrocarbon solvents. UV irradiation of pentane solution of Cp^*_2ReH produced a rapid colour change from yellow to purple.

From the solution could be obtained deep purple crystals of Cp^*_2Re in ca 60 % isolated yield, although the extreme solubility of the compound rendered mechanical losses unavoidable. Cp^*_2Re is a thermally stable air sensitive, purple crystalline solid which is monomeric in solution and in the gas phase.

$$Re + C_5Me_5H \xrightarrow{\substack{condensation \\ at\ 77k}} Cp_2^*ReH$$

$$Cp_2^*\,ReH \xrightarrow{\substack{uv.photolysis \\ in\ pentane}} Cp_2^*Re$$

The electronic and molecular structure of Cp^*_2Re has been studied by X-ray diffraction. The molecular structure is shown in Figure 1 (hydrogen groups have been omitted from the Figure for clarity) with atomic labels.

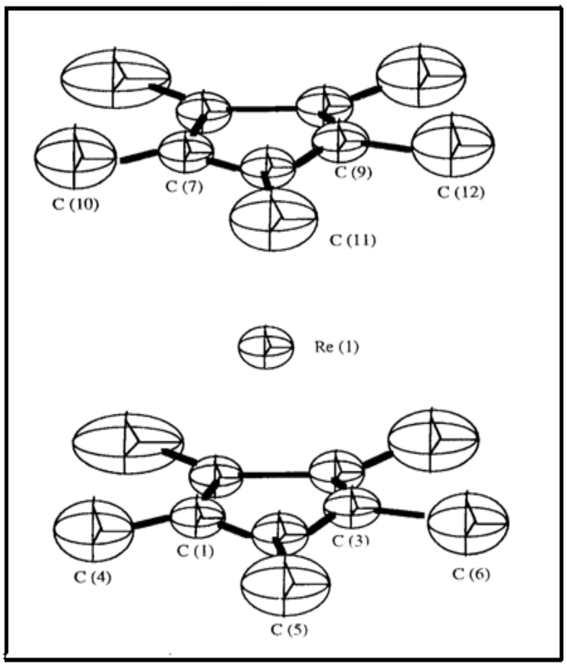

Fig. (1): The structure of Cp^*_2Re[1]

The two cyclopentadienyl rings are planar and parallel with the methyl groups deviating from the ring mean planes by 0.069-0.124Å away from rhenium. Rhenium is found to be 1,882 and 1.880 Å from the mean planes of the two rings and this large separation of the two rings prevents unfavorable methyl-methyl contacts in the eclipsed conformation [1].

The bonding is best treated in the linear combination of atomic orbitals (LCAO - MO) approximation. A semi quantitative energy level diagram is given in figure 2.

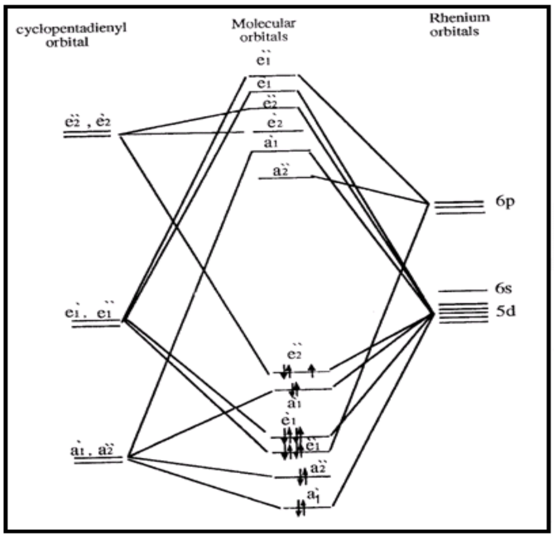

Fig.2: Molecular–orbital energy scheme for Decamethylrhenocene [1]

Each C_5Me_5 ring, taken as a regular pentagon, has five p MOs, one strongly bonding (a), a degenerate pair that are weakly bonding (e_1), and a degenerate pair that are markedly anti-bonding (e_2). The pair of rings taken together then has ten p orbitals.

For Cp^*_2Re, there are seventeen valence electrons to be accommodated, five p electrons from each C_5Me_5 ring and seven valence shell electrons from Re {the electronic structure for Re is [Xe] ($5d^5$) (6s)}. The seventeen electrons can just fill the bonding and nonbonding MOs with one orbital having an unpaired electron.

The five carbon 2pπ AOs form a basis for the representation $a_2'' + e_1 + e_2''$ in the D_{5h} group of cyclopentadienyl, and according to Hückel theory the relative energies of these symmetry orbitals are $e_2'' > e_1'' > a_2''$, as it shown in figure 3

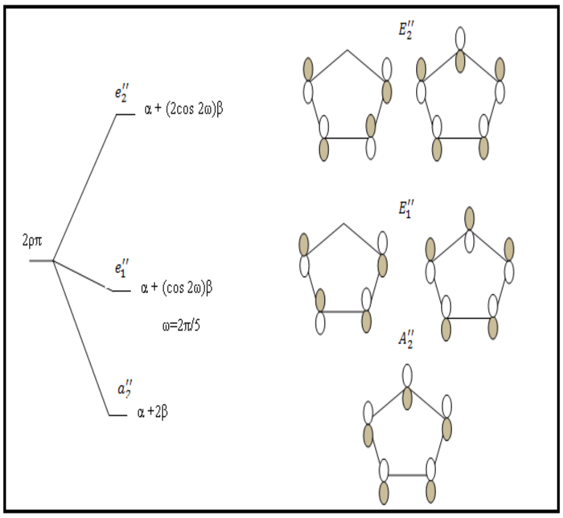

Fig. (3): The molecular orbitals for planar C_5H_5 (point group D_{5h}), [35, 53]

The molecular orbitals for the first ring CpA are [20],

$$CpA(a_2'' \pm) = (5)^{-1/2} \sum_r \phi_r^{(A)}$$

$$CpA(e_1'' \pm) = (5)^{-1/2} \sum_r (\omega^{\pm 1})^r \phi_r^{(A)}$$

Where ω= exp(2πi /5)

$$CpA(e_2'' \pm) = (5)^{-1/2} \sum_r (\omega^{\pm 1})^r \phi_r^{(A)}$$

and the molecular orbitals for the second ring CpB are[20],

$$CpB(a_2'' \pm) = (5)^{-1/2} \sum_r \phi_r^{(B)}$$

$$CpB(e_1'' \pm) = (5)^{-1/2} \sum_r (\omega^{\pm 1})^r \phi_r^{(B)}$$

$$CpB(e_2'' \pm) = (5)^{-1/2} \sum_r (\omega^{\pm 1})^r \phi_r^{(B)}$$

The local molecular orbitals of the first ring, namelyCp_A's, are transformed into the local molecular orbitals of the second ring by the inversion

$Cp_A a$ —>$Cp_B a$, $Cp_A e_1$ —> $Cp_B e_1$.
$Cp_A e_2$—> $Cp_B e_2$

The new orbital's compass both rings to form in this case [20],

1- $Cpa_g = \left(\frac{1}{\sqrt{2}}\right)(Cp_A a + Cp_B a)$,

$$Cpa_u = \left(\frac{1}{\sqrt{2}}\right)(Cp_A a - Cp_B a)$$

2-$Cpe_{1g} = \left(\frac{1}{\sqrt{2}}\right)(Cp_A e_1 + Cp_B e_1)$,

$$Cpa_{1u} = \left(\frac{1}{\sqrt{2}}\right)(Cp_A e_1 - Cp_B e_1)$$

3-$Cpa_{2g} = \left(\frac{1}{\sqrt{2}}\right)(Cp_A e_2 + Cp_B e_2)$,

$$Cpa_{2u} = \left(\frac{1}{\sqrt{2}}\right)(Cp_A e_2 + Cp_B e_2)$$

Since any of these orbitals contain equal admixtures from CpA and CpB, the electron will spend half its time on any one particular ring and the remainder on the other.

Charge -Transfer Spectra

Organometallic compounds exhibit, many of the electronically excited states found in coordination compounds.

The types of excited states in organometallic complexes are as follows [35, 48,49,52]:

Ligand Field Excited States

Low-lying ligand field (L F) or metal-centered excited states of organometallic compounds arise from electronic transitions between the metal d orbital's. As carbon- donor ligands are high in the spectrochemical series, the LF transitions of organometallic complexes are normally observed in the ultraviolet and visible regions and have relatively high energies compared to those of most classical coordination compounds [49-52].

Metal-to-Ligand Charge - Transfer Excited States

Metal to ligand charge transfer (MLCT) states involve electronic transitions from a metal-centered orbital to a ligand-localised orbital. These transitions are commonly observed in organometallic complexes because of the low valent nature of the metal centre and low energy of the acceptor orbital's in many ligands. These transitions may appear in the near infrared, visible or ultra-violet regions [48, 53].

Ligand-to-Met at Charge Transfer Excited States

Ligand to metal charge transfer (LMCT) states involve electronic transition from a ligand-localised orbital to a metal-centered orbital. Due to the fact that carbon donors are high in the spectrochemical series, and this results in large ligand field splitting energies for organometallic systems, many complexes exhibit LMCT states that are fairly high in energy [48, 49].

Metal-to-Solvent Charge-Transfer (MSCT) States

Metal to solvent charge transfer (MSCT) states originate from electronic transitions from metal-centered orbitals to solvent- localised orbitals. In the formal sense these transitions result in oxidation of the metal and reduction of solvent, and the energy of transitions between these states is dependent on the ease of these processes [49].

Metal-to-Metal Charge Transfer Excited States

Metal to metal charge transfer (MMCT) states arise from electronic transitions between metal-centered orbitals of two or more metals. These transitions may appear in the blue or near ultraviolet-regions [53].

Intra-ligand Excited States

Intra-ligand excited states derive from electronic transitions between orbitals that are mainly localised on the ligand [48, 50].

Jet Dynamics

The physics of the seeded jet expansions has been the subject of intense interest, since their discovery as a source of collision-free molecules having a narrow velocity distribution and low rotational and vibrational temperatures [2-4]. However, the full dynamics of the gas jet expansion is complex and a complete mathematical solution covering all regions has not been developed. Adding complexity is the fact that a variety of nozzle designs exist, as discussed by Murphy and Miller [5] and it is clear that such considerations have an influence on important gas dynamical properties such as internal state populations, extent of dimmer formation etc.

A useful summary has been given by Hayes [6] and this provides a useful basis for discussion. Three distinct regions are identified in the expansion process. In the first, the continuum flow region, there are a large numbers of collisions which maintain the isentropic nature of the process and the methods of fluid dynamics may be used to describe this region. Typically, high Reynolds number flow conditions of the order of 10^3 or higher, are used in seeded jets. The second, or transition flow region is one in which the internal degrees of freedom of the molecules begin to fall out of equilibrium and selective cooling takes place. The velocity difference between seeded species and carrier gas has been minimized by acceleration of the former in the continuum region and the cooling of molecules is the result of the differential velocity, or velocity slip, between molecules and the carrier atoms. The third region is termed that of free molecular flow and here the populations of rotational and vibrational states have become fixed. This is the region of interest in collision dynamics experiments and in spectroscopy. It is generally regarded as collision free and therefore the properties of molecules in this region of the expansion will reflect processes that have occurred in the earlier two regions.

A number of properties of the seeded species are used to characterize the expansion process and these include rotational and vibrational temperatures of the seed species (T_{rot}, T_{vib}), velocity distributions, the extent of cluster formation and molecular alignment. It is the latter upon which we focus though note the very significant contributions of Amirav and co-workers [7,8] who demonstrated the importance of acceleration of the seed species to the point where the relative velocity (of seed and carrier) becomes sufficiently low that collisions are cooling rather than heating in nature. The most likely region for this to occur is in the fluid-like region of the expansion where gas densities are at their highest. Amirav and colleagues studied velocities and velocity distribution of heavy molecules seeded into rare gases, as well as their rotational and vibrational temperatures. Other workers have studied the alignment of (mainly diatomic) molecular species and this also will contain information on the gas and/or the fluid dynamics of the expansion process.

Experimental Technique

The apparatus used in the studies have described here in this section.

It is designed to record the spectrum of large organometallic molecules seeded into a supersonic free jet by using laser induced fluorescence (L I F) technique. A schematic diagram of the whole apparatus is given in figure 4.

Briefly, a tunable pulsed dye laser pumped by Nd:Yag laser was used to excite rotationally cooled Cp^*_2Re which was produced by expansion in conjunction with the argon carrier gas through a supersonic nozzle. A Spectron laser system Nd:Yag [Spectron SL, 400) was used to tunable dye laser [Spectrolase 400 DYE LASER]. The Nd:Yag laser was Pockels cell Q-switched with a 8 nsec pulse duration. It produces up to 800mJ of output and has operating wave length of 532 nm. Rhodamine 6G solution in ethanol was continuously pumped through the dye laser and this gave a tuning range of 5820 to 6030 Å emitted as a result of the pumping by the Nd:Yag, the output power was in the region of 250-300 mJ with 10 nsec pulse width.

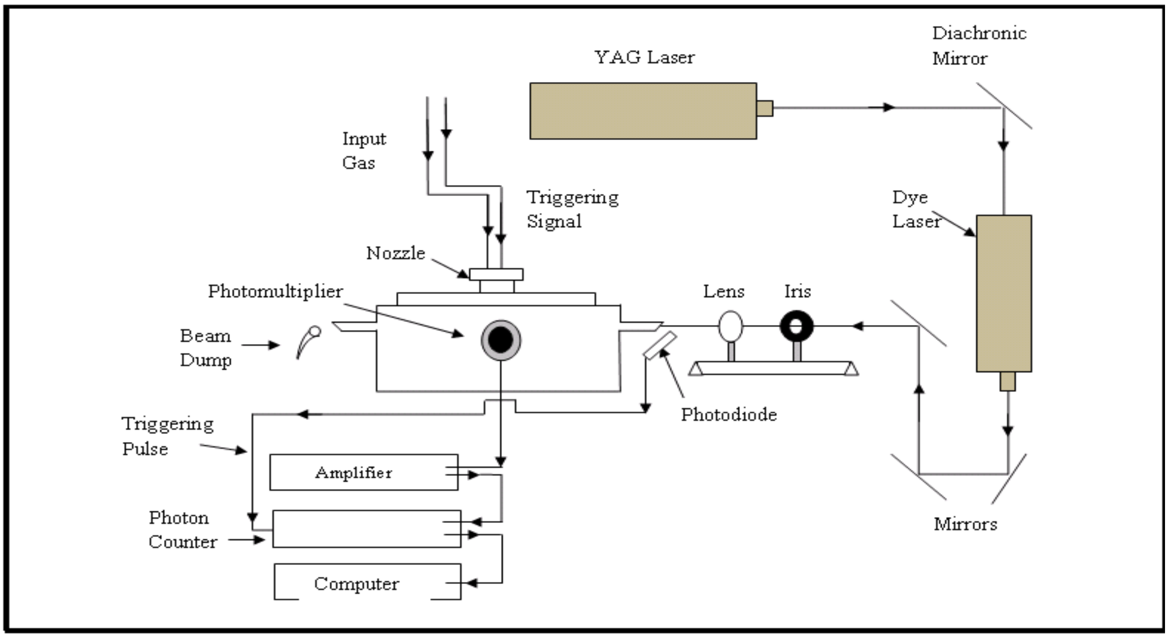

Fig. (4): Experimental design

A mixture of Cp^*_2Re in argon was expanded through a nozzle hole (500µ.m in diameter) into the vacuum chamber. During the experiment the pressure behind the nozzle was 650 torr, and the pressure in the chamber was about $4x10^{-4}$ torr. The background pressure was only $6x10^{-5}$ torr when the molecular beam was cut off. The fluorescence life time of $(\eta^5 - C_5Me_5)_2Re$ is 10 nsec [10.(b)].

The resulting fluorescence is then collected by a bi-convex lens (f=50 mm) fitted inside the chamber. The signal is collected by another bi-convex lens (f= 70 mm) which focuses the light, through a filter (to cut off the unwanted signals), onto the fast photon counting photomultiplier tube (EMI 9863 B/100).

After this the electrical signal is collected by a pre-amplifier which sends the amplified signal to a gated photon counter (Stanford Research System S R 400) which counts the number of photons and sends a signal to a PC where the detected signal going to be monitored. This displays the spectrum as a graph of wavelength against photon counts.

Due to the fact that the large molecules have a low vapor pressure, the sample required heating. However the expansion process ensures that the sample still produced vibrational and rotationally cold molecules in the supersonic expansion at the point of observation.

It is appropriate to mention at this stage that in the case of a large molecule, the spectrum is not expected to show resolved rotational structure in supersonic expansion. If a molecule is large enough the rotational constants are so small that there are many rotational states populated even in very cold molecular beams, and so the spectral lines originating in these several states tend to overlap. Moreover, in a large molecule it is likely that there are many low frequencies, large amplitude vibrational modes and these make the separation of vibration and rotation far from complete. Therefore the supersonic expansions can be useful in the resolution and analysis of vibrational structure of large molecules.

Results and Discussion

The spectrum of the decamethylrhenocene Cp^*_2Re is shown in Figure 5. The spectrum illustrates a high degree of structure, indicating that there are several levels populated and these molecules are able to undergo many possible transitions. A filtration system was introduced in order to ensure the carrier gas is pure enough and contains no impurities such O_2 or H_2O which help to decompose the sample. The inductive effect of the methyl groups is expected to shift the ligand level to high energy resulting in red shift of L M C T and blue shift of M L C T bands. By group theory we know that for a transition to be allowed from the $^2E_{2g}$ ground state it must be to an excited state of $^2E_{1u}$ symmetry. It also has to be polarized in (X,Y) plane (one particular interest of this work is the $^2E_{1u}$ charge-transfer excited state).

An electron is excited from mainly ligand orbitals of odd symmetry, derived from Π orbitals of Cp* ring to predominantly metal 5d levels of even symmetry. These transitions (L —> M) are derived from one electron excitation, from the predominantly ligand e_{1u} level to the e_{2g} hole on the Re atom.

Twelve progressions have been identified and are listed in tables 1—>12, with average interval as follows: (111, 121, 101.5, 94, 81, 143.6, 145.5, 110, 107, 162.3, 162.6, 47) cm^{-1}. They are progressions named A,B,C,D,E,F,G,H,I,J,K and L respectively.

It is a complex spectrum consisting of large numbers of vibronic transitions. It also appeared from the spectra that there are many peaks that over-lap with each other, making the assignment processes very complicated. This is to be expected from a molecule containing 51 atoms which will have 147 vibrational modes (3n-6), the region covered in our spectrum is the long wavelength region of that published by Perutz and co-workers [16]. It falls in a region where there is relatively little structure in the matrix isolated spectra. However, an LIF spectrum (Perutz unpublished result, Figure 6 [28] of dilute Cp^*_2 Re in a matrix of N_2) shows more features in the region of our observation and so a comparison is possible.

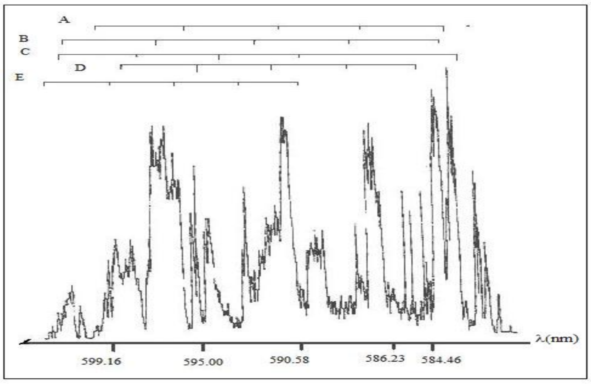

Fig. (5): Laser Induced Fluorescence Spectrum of Decamethylrhenocene

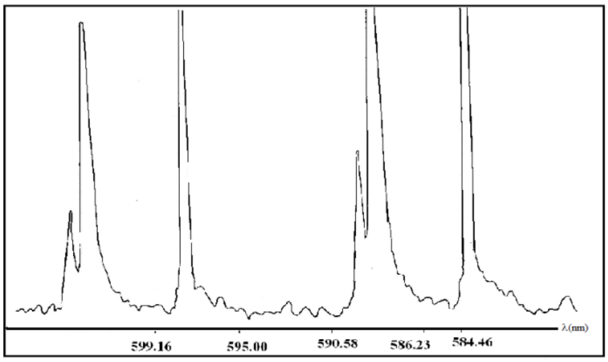

Fig. (6): Laser Induced Fluorescence Spectrum of dilute Cp^*_2 Re in a matrix of N_2

Tables of Progressions

TABLE (9)

PROGRESSION (I)

No	Wavelength/ (nm)	Wavenumber / cm^{-1}	Interval/ cm^{-1}
1	599.02	16694	104 105 111
2	595.30	16798	
3	591.61	16903	
4	587.74	17014	

TABLE(10)

PROGRESSION (J)

No	Wavelength/ (nm)	Wavenumber / cm^{-1}	Interval cm^{-1}
1	601.24	16632	159 163 165
2	595.54	16791	
3	589.81	16954	
4	584.14	17119	

TABLE (11)

PROGRESSION (K)

No	Wavelength/ (nm)	Wavenumber/ cm^{-1}	Interval cm^{-1}
1	598.42	1610.	161 164 163
2	592.72	16871	
3	587.02	17035	
4	581.44	17198	

Table(12)

PROGRESSION (L)

No	Wavelength/ (nm)	Wavenumber / cm^{-1}	Interval/ cm^{-1}
1	601.36	16628	47
2	599.68	16675	45
3	598.06	16720	46
4	596.41	16766	47
5	594.76	16813	47
6	593.11	16860	47
7	591.46	16907	47
8	589.81	16954	48
9	588.16	17002	48
10	586.51	17050	48
11	584.86	17098	48
12	583.21	17146	47
13	581.62	17193	

Tables of Progression

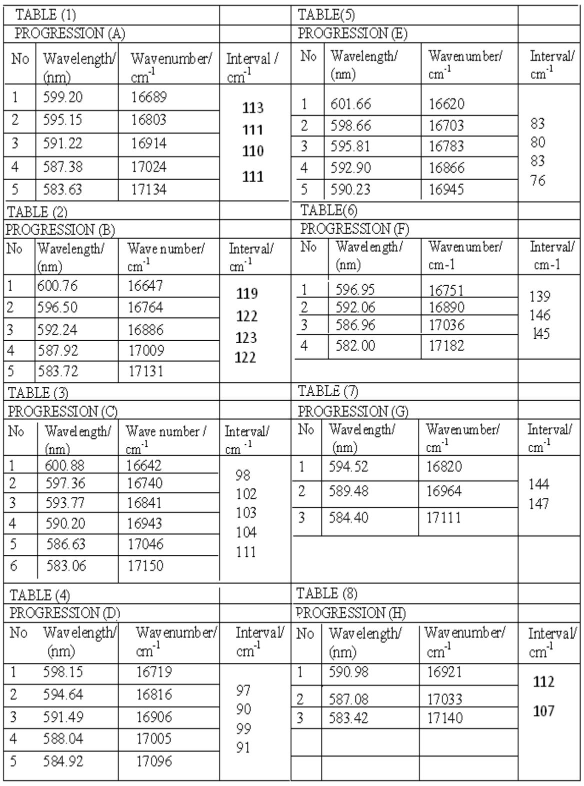

TABLE (1)
PROGRESSION (A)

No	Wavelength/ (nm)	Wavenumber/ cm^{-1}	Interval / cm^{-1}
1	599.20	16689	113 111 110 111
2	595.15	16803	
3	591.22	16914	
4	587.38	17024	
5	583.63	17134	

TABLE (2)
PROGRESSION (B)

No	Wavelength/ (nm)	Wave number/ cm^{-1}	Interval/ cm^{-1}
1	600.76	16647	119 122 123 122
2	596.50	16764	
3	592.24	16886	
4	587.92	17009	
5	583.72	17131	

TABLE (3)
PROGRESSION (C)

No	Wavelength/ (nm)	Wave number / cm^{-1}	Interval/ cm^{-1}
1	600.88	16642	98 102 103 104 111
2	597.36	16740	
3	593.77	16841	
4	590.20	16943	
5	586.63	17046	
6	583.06	17150	

TABLE (4)
PROGRESSION (D)

No	Wavelength/ (nm)	Wavenumber/ cm^{-1}	Interval/ cm^{-1}
1	598.15	16719	97 90 99 91
2	594.64	16816	
3	591.49	16906	
4	588.04	17005	
5	584.92	17096	

TABLE(5)
PROGRESSION (E)

No	Wavelength/ (nm)	Wavenumber/ cm^{-1}	Interval/ cm^{-1}
1	601.66	16620	83 80 83 76
2	598.66	16703	
3	595.81	16783	
4	592.90	16866	
5	590.23	16945	

TABLE(6)
PROGRESSION (F)

No	Wavelength/ (nm)	Wavenumber/ cm-1	Interval/ cm-1
1	596.95	16751	139 146 145
2	592.06	16890	
3	586.96	17036	
4	582.00	17182	

TABLE (7)
PROGRESSION (G)

No	Wavelength/ (nm)	Wavenumber/ cm^{-1}	Interval/ cm^{-1}
1	594.52	16820	144 147
2	589.48	16964	
3	584.40	17111	

TABLE (8)
PROGRESSION (H)

No	Wavelength/ (nm)	Wavenumber/ cm^{-1}	Interval/ cm^{-1}
1	590.98	16921	112 107
2	587.08	17033	
3	583.42	17140	

We find that several of the main features present in the N_2 matrix spectrum are also present in our gas phase spectrum. As anticipated there is considerably more structure in our gas phase spectrum. However, the similarities are sufficient that we are confident that the spectrum shown in Figure 5 is of Cp^*_2Re.

The vibrations can be divided for descriptive purposes into two types: intra-ring modes which can be described as motions within the C_5Me_5 rings, and inter-ring modes which are skeletal movements involving the rings and the metal atom. As it has been mentioned earlier, Cp^*_2Re has altogether 51 atoms and therefore 147 internal vibrations are to be expected. Each ring has [3x25 - 6] 69 ligand vibrations.

There are two ligands, so the total number of the ligand vibrations is 2x69, or 138. Thus the remaining (147-138) =9 normal vibrations are frame work, skeleton, or “inner vibrations’’.

The band assignments could be considered under three headings:

(1) The methyl groups.

(2) Cp* ring, with methyl groups as point mass.

(3) The Cp^*_2Re groups and the modes involving movement of each ring against Cp*Re fragments. Methyl groups vibrations, for many Cp* molecules, bands of medium intensity are observed [29] in the 3000-2000, 1500-1450, and 1050-1000 crn^{-1} regions, which can be ascribed to A_1 and E species ν (CH_3), δ(CH_3) and ρ (CH_3) modes respectively. The expected normal modes for C_5Me_5 ring with D_{5h} local symmetry are the following [29]: three stretching C-Me vibrations, ν CMe(A_1'+W_1+E_2); three ring vibrations, ν CC(A_1'+E_1'+E_2'); three-out-of plane CMe bending vibrations, δCMe(A_1''+E_1'+E_2'); in-plane ring deformation, δCC (E_2') and out-of-plane ring deformations, γCC(E_2').

A medium strong band at 1390 cm^{-1} was assigned to the CC stretching vibration of the E_1' species by Diaz et al. [29]. This normal mode is frequently observed for Cp-derivatives in the 1400-1500 cm^{-1} region [30, 31]. Furthermore, a similar assignment was proposed by Parker et al. [32], while Lokshin et al. [33] in a vibrational study of $Cp^*Re(CO)_3$ have ascribed this vibration to a band at 1420cm^{-1}. A strong band at 1103 cm^{-1} has been assigned by Lokshin et al. [33] to the A_1', ring breathing vibration. The C-Me stretching (E_1') is placed at 1230 cm^{-1} for Cp-Me by Parker et al. [32]. Those vibrations attributed to in-plane δ(CMe) and out-plane γ(CMe) bending are expected in the region below 400 cm^{-1}. In this respect a weak band at ca 350 cm^{-1} has been assigned by Dias et at. [29] to δ(CMe) by comparison with the spectrum of (MeC_5H_4) $Mn(CO)_3$ [32] and assignments made for toluene [34, 35] and dimethylferrocene [29]. The δ(CMe) bending has appeared at lower energy, and it is observed as weak bands at ca 290, 270, 250, and 230 cm^{-1} by Diaz et al. [29]. In the case of skeleta1 modes, it should be taken into consideration that the skeletal modes depend considerably upon the metal and the nature of the compound. The ligands are regarded as rigid disks when the skeletal or inner vibrations are to be determined. As already has been calculated there are 9 normal vibrations modes of skeletal or inner vibrations. The expected normal modes for Cp^*_2Re with D_{5h} local symmetry are listed as follow [31]:

Type of vibration	Irreducible representation
Symm. metal-ring stretch	A_1'
Torsion	A_1''
Asymm. Metal-ting stretch	A_2''
Symm. ring tilt	E_1''
Asymm. ring tilt	E_1'
R-M-R deformation (Cp*-R-Cp*)	E_1'

Figure 7 illustrates schematically these nine normal vibrational modes. The two fold degenerate modes are shown with only one component. The A_1 Cp*-Re stretch band has been reported to be weak and the E_1 ring tilt band, as a rule, is found at higher frequency than the A_1bands.

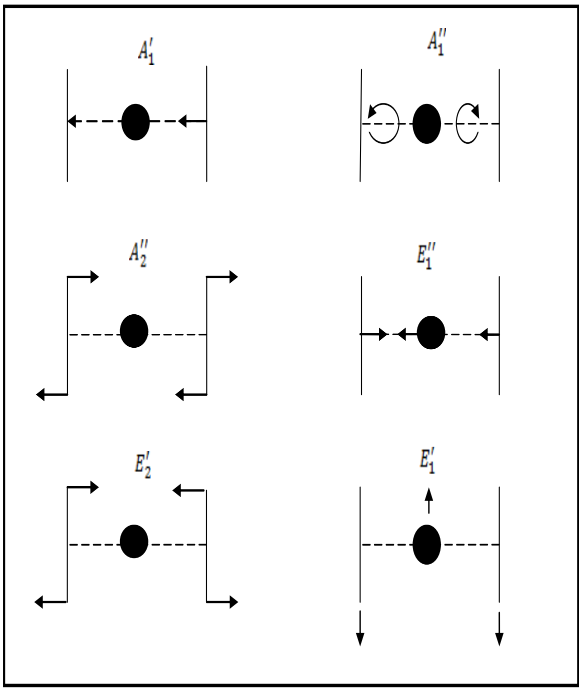

Fig. (7): Normal vibration for skeletal modes.

Otherwise it has been noted that the ring-tilt is shifted to higher energy when methyl groups are substituted on the ring. This trend is observed in $MeC_5H_5Mn(CO)_3$ [32] and dimethylferrocene [37]. Characteristic absorptions assigned to those normal modes have been observed at 349 and 327 cm^{-1} for $CpRe(CO)_3$ [33] at 372 and 354 cm^{-1} for $CpMn(CO)_3$ [38] and at 388 and 354 cm^{-1} for $MeC_5H_4Mn(CO)_3$ [32]. On the other hand, these vibrations have been placed at 380 and 360 cm^{-1} for $CpMo(CO)_3I$ and at 370 and 348 cm^{-1} for $CpFe(CO)_2C1$ [39].

On the basis of the above data and the outlined trends, a weak doublet was assigned by Diaz et al. to the ring-tilt mode, at ca 370 cm^{-1} for $Cp^*Re(CO)_2\ C1_2$ [29], whereas the very weak band at ca 290 cm^{-1} was tentatively ascribed to the Cp*-Re stretching. The low value of this frequency can be justified by the increased mass of the Cp* ring.

For torsion and Cp*-Re-Cp* deformation, we have no data available to assign these two vibrational modes and at what frequency they would occur, what we could know of the expected frequency of these two modes is from their assignment in similar compounds such as Cp_2Fe and Cp_2Ru where they are found at very low frequency [41]. Adams et al. [40], reported results on Ruthenocene, and has assigned the ca 130-138 cm^{-1} band is due to torsion and he also assigned ca 165-172 cm^{-1}bands to be (ring-Ru-ring) deformation.

The assignment of frequencies corresponding to torsion and Cp*-Re-Cp* deformation could be facilitated more by looking at the frequencies of other skeletal vibration modes [tilt and stretch] and making simple comparisons with the similar modes in Cp_2Ru and Cp_2Fe.

In Ruthenocene, Bodenheimer and Low [41] have assigned the tilt and ring stretch modes to frequencies 400cm^{-1} and 333cm^{-1} respectively, whereas the assignments of similar modes in Ferrocene were 389 cm^{-1} and 309 cm^{-1} respectively. The corresponding frequencies for these modes in Cp^*_2Re were assigned to 370 cm^{-1} and 290 cm^{-1} respectively.

On this basis, by taking into account the mass of the Re atom which is less than twice that of the Ru atom and also by taking into consideration the following:

1- The increasing mass of the Cp* ring which that could lead to a lower frequency [29].

2- A large separation of the two rings from the Re atom, where the Rhenium atom is found to be 1.882Å and 1.880Å from the mean planes of the two rings (1), one might predict the approximate frequency at which these vibrational modes could be expected.

By inspecting the frequency assignments of Cp^*_2Re spectra, no progression corresponding to the methyl groups and the Cp* rings has been observed. Our observations were limited by the restricted tuning range of the exciting laser, (16556—>17182) cm^{-1}.

In the case of skeletal vibration modes, for the same reason as above, no progression has been observed or assigned corresponding to the tilt or ring-stretch modes.

In comparison with ruthenocene and ferrocene [40, 41], we assigned the frequencies 162.3 cm^{-1} and 162.6 cm^{-1} as corresponding to Cp*-Re-Cp* deformation and the frequencies 143.6 cm^{-1} and 145.5 cm^{-1} corresponding to torsional motion. In the meanwhile, from the Cp^*_2Re spectra, we obtained a number of progressions with frequency, less than 100 cm^{-1}.

We have no available information with which to assign these bands at present.

Limitations of Jet Spectroscopy

As it has mentioned earlier, the advantage of the jet technique is the ability to produce a beam of molecules that are vibrational and rotationally cold yet still a vapor. However, before that can happen the molecule must be vaporized. Hayes and Small [42] noted that in a continuous expansion of a complex mixture the intensity of a peak in the laser induced fluorescence spectrum is proportional to the vapor pressure in the reservoir of the component responsible for that absorption. However, the partial pressure of each component can depend upon the partial pressure of other species in the mixture and partial pressures are subject to change during the course of an experiment as the component becomes diluted in the reservoir. In addition to the design constraints imposed by high temperature operation, such species are often thermally labile and cannot be vaporised by the simple expedient of increased heating. This problem is exacerbated by catalysis of decomposition due to materials used to construct a high temperature apparatus

References

[1] J. Bandy, F. Clock, G. Cooper, J. Day, R. Girling, R. Graham, J. Green, R. Grinter and R. Perutz, *J. Am. Chem*. Soc., 1 10, 5039 (1988).

[2] A. Kantrowitz and J. Grey, *Rev. Sci. Instr.* ***22***, 328 (1951).

[3] T. A. Milne and F. T. Green, *Adv. High Temp. Chem*. **2**,107 (1969)

[4] J. B. Anderson, R. P. Andres and J. B. Fenn, *Adv. Chem. Phys*. ***10***, 275 (1963).

[5] H. Pauly and J. P. Toennies, *Meth. Exp. Phys*., *7*A, 227 (1968).

[6] H. R. Murphy and D. R. Miller, *J. Phys. Chem*., ***88***, 4474 (1984).

[7] J. M. Hayes, *Chem. Rev.* 87, 745 (1987).

[8] A. Amirav, U. Evan and J. Jortner, *Chem. Phys*., ***51***, 32 (1980).

[9] J. M. Hollas, D. Phillips, Jet Spectroscopy and Molecular Dynamics, Springer Netherlands (1995).

[10] a) P., Cox, P. Grebenik, R. Perutz, R. Graham, R. Grinter, *Chem. Phys. Lett.,* ***5***, 415 (1984).

b) S. Bell, J. Hill, A. McCamley and R. Perutz, *Pure and Appl. Chem.* 62(8), 1539 (1990).

[11] A. Haaland, *Acc. of Chem. Res.,* ***12***, 415(1979)

[12] S. Evan, M. Green, B. Jewitt, A. Orchard, C. Pygall, *J. Chem. Soc., Faraday Trans*., ***68***(2), 1847 (1978).

[13] P. Grebenik, R. Grinter, R. Perutz, *Chem. Soc. Rev.*, ***17***, 453 (1988).

[14] J. Chetwynd-Talbot, P. Grebenik, R. Perutz, M. Powell, *Inorg. Chem.*, ***22***, 1675 (1983).

[15] J. Chetwynd-Talbot, P. Grebenik, R. Perutz, *Inorg. Chem*., ***21***, 3647 (1982).

[16] D. Haddleton, A. McCamley, R. Perutz, *J. Am. Chem. Soc.*, ***110***, 1810 (1988).

[17] S. Evans M. Green , B. Jewitt, G. King, A. Orchard, *J. Chem. Soc., Faraday Trans*. ,***70*** (2), 356 (1974)

[18] D. Duggan , D. Hendrickson, *Inorg. Chem.*,14(5), 955 (1975).

[19] K. Gordon, K. Warren, *Inorg Chem*., ***17***(4), 987 (1978).

[20] A. Liehr, C. Ballhausen, *Act. Chem. Scand*., ***2***, 207 (1957).

[21] W. Moffitt, *J. Am. Chem. Soc*., ***74***, 3386(1954).

[22] H. Jaffe, *J. Chem. Phys.*, ***2l*** (l),!56 (1953).

[23] A. Lees, *Chem., Rev.*, ***87***, 711(1987).

[24] L. E. Orgel, *J. Chem. Phys.*, ***23***(6), 1004, (1955).

[25] F. G. N. Cloke, A. N. Dix, J. C. Green, R. N. Perutz, E. A. Seddon, Organometallics ***2***, 1150 (1983).

[26] P. Pasman, J. Snel, *J. Organomet. Chem.*, 276, 387(1984).

[27] M. Green, G. Wilkinson, *J. Chem., Soc.*, 4314 (1958).

[28] R. Perutz, Unpublished results.

[29] G. Diaz et al., *Polyhedron*, ***7***, 24, 2743 (1988).

[30] I. J. Hyams, R.T. Bailey and E. R. Lippincott, *Spectrochim Acta*, 23A, 273 (1967).

[31] H, P. Fritz, Adv. *Organometal. Chem*., 1, 239, (1964).

[32] D.J. Parker and M. H. B. Stiddard, *J. Chem. Soc.*, 1040, A, (1970).

[33] B.V. Lokshin, Z. S. Kleemkova and Yu.V. Makarov, *Spectrochim Acta*, 28A, 2206, (1972).

[34] J. K. Wilmshurst and H. J. Bernstein, *Can. J. Chem.*, ***35***, 911 (1957).

[35] R. H. Silverstein, G. C. Bassler and T. C. Morrill, *Spectrometric identification of Organic Compounds.* John Wiley, New York (1974).

[36] R.T. Bailey and E. R. Lippincott, *Spectrochim Acta*., ***21***, 389 (1965).
[37] N. Fuson, C. Garrigou-Lagrange and M. L. Josien, *Spectrochim Acta*, ***16***, 106 (1960).
[38] D. J. Parker, Ph.D. Thesis, University of London (1968).
[39] D. J. Parker, *J. Chem. Soc*, 1382, A (1970).
[40] D. M. Adams and W. S. Fernando, *J. Chem. Soc. Dalton*, 2507 (1972).
[41] J. S. Bodenheimer, and W. Low, *Spectrochim Acta*, 29A, 1733 (1973).
[42] J. Hayes, G. Small, *Anal Chem*., ***54***, 1202 (1982).
[43] M. Ito, T. Ebata, and N. Mikami, *Anal. Rev. Phys. Chem*., ***39***, : 123-147 (1988).A.
[44] Amirave, U. Evan and J. Jortner. *Bull. Soc. Chim. Belg*. 92/n^o, 6-7 (1983).
[45] E. Kolodney and A. Amirav, *Chem. Phys*. ***82***, 269 (1983)
[46] T. Imasaka et. al., *Pure Appl. Chem*., ***75***, 975-998 (2003).
[47] A. Amirave, U. Evan and J. Jortner, *Anal. Chem*. ***54***, 1666-1673 (1982).
[48] H. Yersin, Transition Metal and Rare Earth Compounds III: Excited States, Transition, Interactions, Springer-New York (2004).
[49] G.S. Mankue, Theoretical Principle of Inorganic Chemistry, Tata McCGraw-Hill Education (2006).
[50] Dr. B. K. Sharma, Spectroscopy, GOEL-Delhi (2007).
[51] K. Nakamoto, Infrared and Raman Spectra of Inorganic and Coordination Compounds John Wiley & Sons, New Jersey (2009).
[52] Thomas Schönherr, Optical Spectra and Chemical Bonding in Transition Metal Complexes, Springer-New York (2004).
[53] K. Reddy, Symmetry And Spectroscopy Of Molecules, New Age International-New Delhi (2005).

تأثير الليزر على طيف الفلورة لمركب الديكاميثل رومين في النفاث الفوق السمعي

حارث جميل صالح

معهد الليزر للدراسات العليا ، جامعة بغداد ، بغداد ، العراق

الخلاصة: في البحث تم أستخدام تقنية Supersonic Jet Laser Induced Fluorescence Spectroscopy, وهي عملية تعجيل جزيئات المادة الى سرعة الصوت بواسطة غاز حامل لذرات تللك المادة ومن ثم دراسة الطيف المنبعث منها بعد تهيجها بواسطة الليزر. هذه التقنية تسهل عملية دراسة أطياف المركبات العضوية المعدنية والسندويجية التركيب والتي تتألف من عدد كبير من الذرات وخاصة الميتالوسينية. عمليات انتقال الشحنة في هذه المركبات وخاصة انتقال الشحنة من اليكند (ligand) الى المعدن (metal) في Decamethylrhenocene $(\eta^5 - C_5 Me_5)_2 Re$ هو موضوع بحثنا واهتمامنا. بعد تهيج هذا المركب بالليزر أظهر طيفها درجات عالية من التركيبات والتي تشير الى ان هذا المركب العضوي قد اشغل مستويات عدة من الطاقة وأن هذه الجزيئات ممكن أن تخضع لأنتقالات متعددة بين مستويات الطاقة.